A single channel capillary microviscometer

N. Morhell & H. Pastoriza

Microfluidics and Nanofluidics

ISSN 1613-4982
Volume 15
Number 4

Microfluid Nanofluid (2013) 15:475-479
DOI 10.1007/s10404-013-1162-4

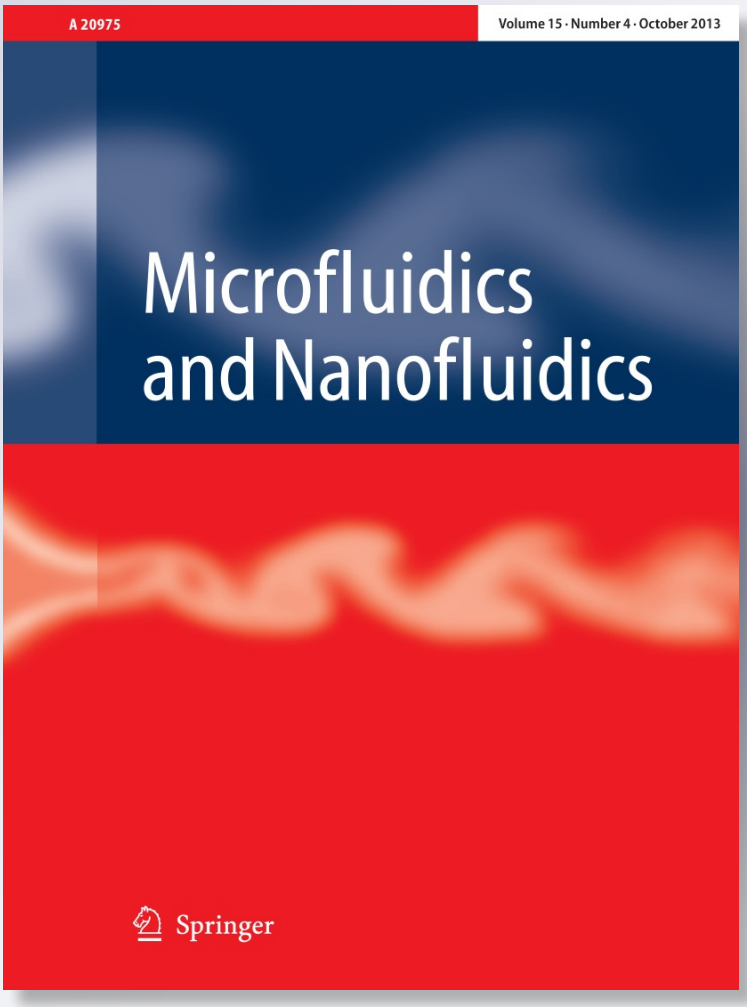

Springer

Microfluid Nanofluid (2013) 15:475–479
DOI 10.1007/s10404-013-1162-4

RESEARCH PAPER

A single channel capillary microviscometer

N. Morhell · H. Pastoriza

Received: 23 November 2012 / Accepted: 19 February 2013 / Published online: 12 March 2013

Abstract We have developed a microviscometer analyzing the fluid dynamics in a single channel glass microfluidic chip with a closed end. The device is able to test sample volumes of a few microliters by inserting one drop in the inlet. The fluid enters the channel driven by capillary pressure and an optical sensor registers the motion. The equation that describes the fluid dynamics is function of the channel geometry, atmospheric pressure, fluid viscosity, and capillary pressure. Knowing the first two, the last parameters can be obtained as fitting parameters from the meniscus position as a function of time plot. We have successfully tested Newtonian fluids with different viscosities and capillary pressure.

Keywords Microviscometer · Glass micromachining · Closed channel

1 Introduction

In the past 10 years, several developments of viscosity sensors using microfluidic chips have been reported by Han et al. (2007), Chevalier and Ayelaa (2008), and Lee and Tripathi (2005). The chips's main feature of using small amount of fluid (≈1 μL) for sample testing makes these microviscometers quite attractive for clinical analysis purposes, as well as in applications such as ink, oil, food, and pharmaceutical industries.

Viscometers has been built using different working principles: from flows established by optically rotating particles (Parkin et al. 2007), hydrodynamic focusing (Nguyen et al. 2008), to miniaturizing the capillary viscometers using microchannels. In their review, Pipe and McKinley (2009) discuss many works about microfluidics rheometry, and two kinds of approaches were highlighted. The first one analyzes the fluid dynamics by setting a pressure difference and measuring the flow rate or velocity. The second approach fixes a flow rate and measures the resulting pressure difference. Following the first, Srivastava et al. (2005) and Srivastava and Burns (2006) reported the fabrication of a microviscometer using the capillary pressure as a driving force of a fluid. The working principle is based on measuring the meniscus position as a function of time for a liquid entering an open microchannel driven only by capillarity. With both ends of the microchannel at atmospheric pressure, a fully developed Poiseuille is established and the liquid viscosity can be obtained. However, an independent and reliable measurement of the capillary pressure must be obtained. In their work, Srivastava et al. obtain this value measuring the final position for the liquid entering a second channel with a closed end. The fluid enters the closed channel by capillarity until the air pressure inside equals the atmospheric plus the capillary pressure. Thus by knowing the channel geometry, the rest position of the fluid column is directly related to the capillary pressure.

The dynamic of a fluid entering a closed channel also depends on the viscosity μ and the capillary pressure. Therefore, by studying these dynamics, the parameters could be directly obtained. Following this idea, we present

N. Morhell: Fellowship holder Consejo Nacional de Investigaciones Científicas y Tecnológicas (CONICET)
H. Pastoriza: Researcher at Consejo Nacional de Investigaciones Científicas y Tecnológicas (CONICET)

N. Morhell · H. Pastoriza (✉)
Comisión Nacional de Energía Atómica, Laboratorio de Bajas Temperaturas, Centro Atómico Bariloche and Instituto Balseiro, (R8402AGP), S. C. de Bariloche, Argentina
e-mail: hernan@cab.cnea.gov.ar

N. Morhell
e-mail: nadimest@gmail.com

in this work both theory and experiment of a liquid drop entering a closed microchannnel and its application as a viscometer.

2 Theory: transient flow in a closed microchannel

The transient analysis of a capillary driven fluid entering a closed nanochannel was studied by Phan et al. (2010) and independently by Radiom et al. (2010) using a parameter which implicitly contained information about the capillary pressure. Here, we present the model and the solution by explicitly showing the viscosity μ and capillary pressure P_c as fitting parameters.

When a Newtonian fluid is set to a pressure gradient dP/dx across a microchannel of hydraulic diameter d, a Poiseuille flow with a parabolic velocity distribution is established. It is well-known that the mean velocity v depends only of d, μ, and dP/dx, and is given by

$$v = \frac{dx}{dt} = \frac{d^2}{8\mu}\frac{dP}{dx} \tag{1}$$

For low velocities, the dynamic pressure drop can be neglected (White 1998) and dP/dx can be written just as a difference of hydrostatic pressures over the fluid length x. In this case, $dP/dx = \Delta P/x$. Considering a channel of length L with a close end, $\Delta P = P_1 - P_2$ with P_1 and P_2, the pressures at the points shown in Fig. 1. The air P_2 inside the channel is initially at atmospheric pressure P_0 and increases as the fluid enters into the channel. Considering an isothermal process, it can be seen that P_2 goes as

$$P_2 = P_0\frac{L}{L-x} \tag{2}$$

As for P_1, the contribution of both atmospheric and capillary pressure P_c is considered. P_c depends mainly on the channel geometry, the surface tension γ, and the contact angle θ, given by

$$P_c = \frac{\gamma}{d}cos(\theta) \tag{3}$$

The fluid enters the channel (Fig. 2) until it stops at a final equilibrium position L_f where $P_2 = P_1 = P_c + P_0$.

$$P_0 + P_c = P_0\frac{L}{L-L_f}$$

$$P_c = P_0\frac{L_f}{L-L_f}$$

Finally, the differential Eq. 1 can be rewritten as

$$\begin{aligned}\frac{dx}{dt} &= \frac{d^2}{8\mu x}(P_0 + P_c - P_2(x)) \\ &= \frac{d^2}{8\mu}\frac{P_0 L}{(L-L_f)}\frac{(L_f - x)}{x(L-x)}\end{aligned} \tag{4}$$

Fig. 1 Schematic of a fluid entering closed channel by capillary pressure. *Region 1* fluid, *region 2* trapped gas

and can easily be integrated considering the initial conditions $x = 0$ at $t = 0$. Thus,

$$t = \frac{8\mu}{d^2}\frac{(L-L_f)}{P_0 L}\left[\frac{x^2}{2} - (L-L_f)\left(x + L_f\ln(1-\frac{x}{L_f})\right)\right] \tag{5}$$

This expression gives the time that it takes the fluid to travel a distance x inside the channel. The logarithmic divergence at $x = L_f$ represents the rest position of the fluid inside the channel achieved when the capillary pressure equals the pressure increase in the gas confined in the channel.

For increasing the fluid viscosity, the dynamics slows down and the curvature increases as seen in Fig. 2a. As expected, for a given viscosity, the fluid goes deeper into the channel as the capillary pressure increases as is shown in Fig. 2b. Therefore, given a channel geometry, the viscosity and L_f can be obtained as the fitting parameters of the nonlinear Eq. 5 with no need of independently measure P_c.

For very large channels ($L_f \gg x$), the early regime is essentially a capillary filling in an open channel, a phenomena that has been widely understood using the Lucas-Washburn equations (Washburn (1921)); Lucas (1918) featuring a $x \propto \sqrt{t}$ relation, which is a solution for a fully developed Poiseuille flow. It can be easily shown in Eq. 5 that for $\frac{x}{L_f} \to 0$, $\ln(1-\frac{x}{L_f}) \sim -\frac{x}{L_f}$, and the linear terms get canceled resulting in a $t \propto x^2$ relation, as expected for a capillary filling.

The model for closed channel filling was derived from a viscous and fully developed Poiseuille flow. Very recently, Das et al. (2012) address the problem of capillary filling and show that inviscid flow is dominant for $x \sim d$. As these authors point out, the viscous-free regime can be observed for times lower than $\tau_c = \sqrt{\rho R^3/\gamma}$, where ρ is the fluid density, γ the surface tension, and R the hydraulic diameter. For our micron sized channels, $\tau_c \approx 5 - 10\,\mu s$ using values of typical fluids. This value is below the time resolution of our current hardware.

3 Experimental details

To test the single channel design, we built microchannels in soda lime glass using photolithography and glass etching

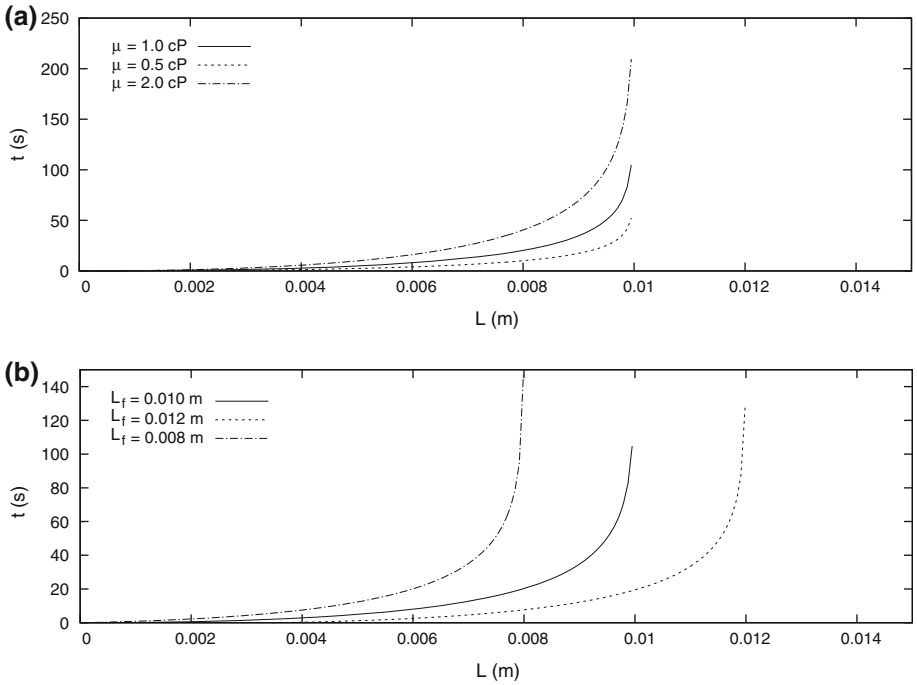

Fig. 2 **a** Numerical solution of Eq. 5 for a given viscosity and channel length for different capillary pressures. **b** Solutions of Eq. 5 for a given capillary pressure and channel length and different fluid viscosities

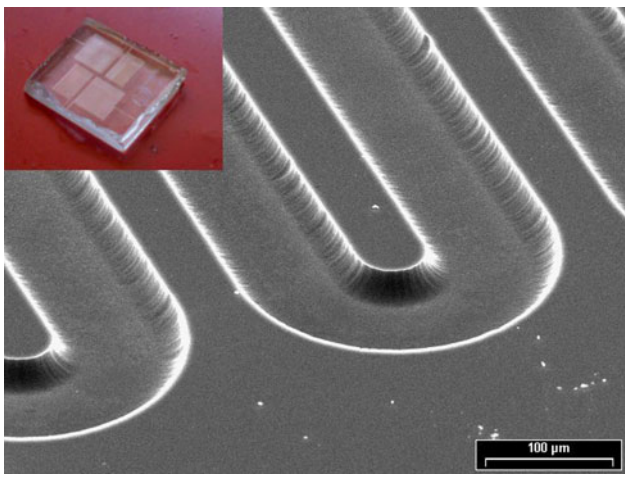

Fig. 3 Scanning electron microscope image of a region of the etched glass slides. *Scale bar* of 100 μm. The *inset* shows an optical image of the finished device

techniques. A drop of fluid sample was inserted on the inlet and the channel got partially filled by capillarity. The motion of the fluid column was recorded using a generic USB Microscope. An image processing software registered the $t(x)$ dependence from which the viscosity was obtained after a non-linear fitting procedure.

3.1 Microchannels fabrication

We fabricated 50 μm width microchannels etching a soda lime glass slide covered by a patterned mask. Several masking methods and etchants solutions have been reported in the literature by Alvares et al. (2008). In our case, we obtained the best results using a chromium hard mask and a Buffered Oxide Etchant (BOE).

Microscope glass slides (76.2 mm × 25.4 mm) were first cleaned using acetone, isopropanol, and DI water in an ultrasonic bath. Then a 500-nm chromium film was sputtered in an argon pressure of 10 mTorr. A positive resist AZ9260 was spun at 2,400 rpm for 60 seconds and soft baked at 106 °C for 2 min. After a 10 min rehydration in a humid atmosphere, we illuminated the resist using a SUSS MJB4 Mask Aligner through the designed mask and developed for 4 min using the AZ400k Developer. Chromium was etched with a solution of 20 gr.$(NH_4)_2Ce(NO_3)_6$, 3.5 ml of acetic acid and 97.5 ml of DI water. After 100 minutes of glass etching with BOE (5 % BHF (NH_4F:HF 7:1), 10 % HCl and 85 % H_2O), a channel height of 15 μm was obtained (Fig. 3). The channels were sealed with another glass slide via fusion bonding at 620 C for 5 hours.

3.2 Videomicroscopy

A custom processing software were build using the Open Computer Vision Library to obtain the meniscus position as a function of time from the captured video. The main algorithm was based in a background subtraction where the fluid column would be the only relevant feature of the image. An array of checkpoints were defined on the image where the intensity of the subtracted image was evaluated for each video frame. The time when the fluid crossed a checkpoint position was recorded. Threshold for

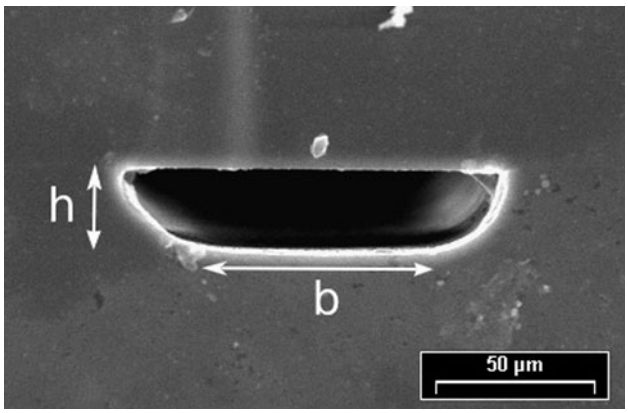

Fig. 4 Scanning electron microscope image of a cross section of a finished channel

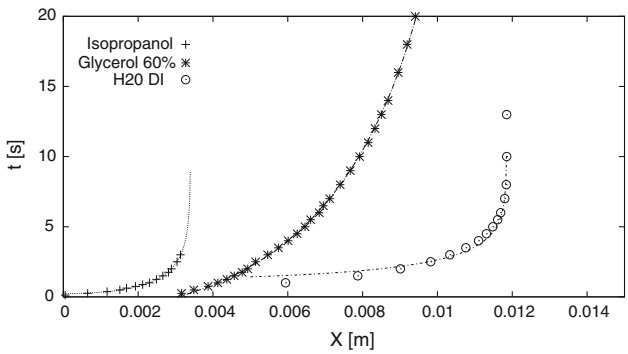

Fig. 5 Time as a function of position for different fluids entering the microviscometer device. *Lines* indicate the fit of Eq. 5 to the data values

Table 1 Viscosity of test fluids measured with the single channel design and the contrast with the commercial Brookfield Rotational model

Viscometer: Sample	Single channel Viscosity (cP)	Brookfield rotatory Viscosity (cP)
DI water	0.98 ± 0.01	0.99 ± 0.01
Isopropanol	1.76 ± 0.02	1.76 ± 0.02
Glycerol 60	7.7 ± 0.2	7.6 ± 0.1

background subtraction and and trigger level at checkpoints were tuned in each case depending on the fluid transparency and the local illumination. Using a previous pixel to length calibration, the t vs x plots were fitted by the non-linear Eq. 5 using a Levenberg–Maquard algorithm.

4 Results

We calibrated the microchannels depth as a function of time left in the BOE etchant, obtaining 0.15 μm/min and a final depth of 15 μm after 100 min (Fig. 3). These values were taken by white light optical profilometry using a Veeco Wyko NT1100 system. The SEM images of a transverse cut (Fig. 4) shows a round trapezoid section typical of a wet isotropic etching processes. The hydraulic diameter, d, of these sections can be calculated as a

$$d = 2h\frac{b/h + \pi/2}{b/h + \pi/2 + 1},$$

where b and h are the channel's base width and depth, respectively (Nguyen 2006).

A single microchannel was tested with DI Water, Isopropanol, and a 60 % Glycerol solution. Then, we fitted Eq. 5 fixing L and $P_0 = 930$ hPa (barometric pressure at the lab) and using μ, L_f, and a time offset t_0 as free parameters. Figure 5 shows both measured and fitted data in an x vs t plot. Viscosity values are shown in Table 1. The samples were also measured with a commercial Brookfield Rotational Microviscosimeter.

The viscosity values measured with the single channel design match those tested taken with the commercial rotational viscometer.

If DI water went deeper into the channel, then it's capillary pressure was the highest. This is an expected result considering that water has a surface tension of 72.88 mN/m, Isopropanol (21.32 mN/m), and Glycerol (41.8 mN/m) (Jasper 1972).

5 Discussion: validity of the model

Equation 3 is deduced considering a static equilibrium of the solid-water-gas interface. When the fluid is in motion due to an external force, the contact angle changes to allow to establish a new equilibrium of forces (Marsh et al. 1993; Radiom et al. 2010).

A velocity dependent contact angle γ should be added to Eq. 3, and the capillary pressure P_c term would be replaced a sum of a static component $P_{c-static}$ and a dynamic component $P_{c-dyn}(dx/dt)$. Several models have been proposed for the description of the dynamic contact angle. Saha and Mitra (2009) have revised these models and compared with numerical calculations and experimental data. One of the conclusions of their extensive work is that the dynamic contact angle had very minor effect on the capillary flow in microchannels. Similar conclusions have been obtained by Waghmare and Mitra (2012). Our data can be adjusted with high confidence by the equation presented in this paper for different static contact angles and fluid viscosities. From our results, we can conclude that the effect of a dynamical contact angle would be relevant only during the initial fluid entrance into the microchannel were high velocities and a no fully developed velocity profile are expected.

6 Conclusions

Single channel microfluidic chips for fluid viscosity measurements were built and tested. We show that from the analysis of the transient response of the fluid entering by capillarity in a single ended channel the fluid viscosity can be obtained directly. Unlike other microfluidic chip viscometer models, our design with a single channel can measure both viscosity and capillary pressure as the device also works as a manometer.

The precision relies mainly in the image processing resolution, and mastering the microfabrication technique to get reproducibility in geometrical dimensions.

References

Alvares MC, Ayuso DP, Granda MG (2008) Critical points in the fabrication of microfluidic devices on glass substrates. Sensors Actuat B 130:436–448. doi:10.1016/j.snb.2007.09.043

Chevalier J, Ayelaa F (2008) Microfluidic on chip viscometers. Rev Sci Instrum 79:076–102. doi:10.1063/1.2940219

Das S, Waghmare PR, Mitra SK (2012) Early regimes of capillary filling. Phys Rev E 86:067–301. doi:10.1103/PhysRevE.86.067301

Han Z, Tang X, Zheng B (2007) A PDMS viscometer for microliter Newtonian fluid. J Micromech Microeng 17:1828–1834. doi:10.1088/0960-1317/17/9/011

Jasper JJ (1972) The surface tension of pure liquid compounds. J Phys Chem Ref Data 1(4):841–1010. doi:10.1063/1.3253106

Lee J, Tripathi A (2005) Intrinsic viscosity of polymers and biopolymers measured by microchip. Anal Chem 77:7137–7147

Lucas R (1918) Ueber das zeitgesetz des kapillaren aufstiegs von flssigkeiten. Kolloid-Zeitschrift 23:15–22. doi:10.1007/BF01461107

Marsh JA, Garoff S, Dussan V EB (1993) Dynamic contact angles and hydrodynamics near a moving contact line. Phys Rev Lett 70:2778–2781. doi:10.1103/PhysRevLett.70.2778

Nguyen NT (2006) Fundamentals and Aplications of Microfluidics. Artech House integrated microsystems series, Artech House

Nguyen NT, Yap YF, Sumargo A (2008) Microfluidic rheometer based on hydrodynamic focusing. Meas Sci Technol 19(8):085–405. doi:10.1088/0957-0233/19/8/085405

Parkin SJ, Knöner G, Nieminen TA, Heckenberg NR, Rubinsztein-Dunlop H (2007) Picoliter viscometry using optically rotated particles. Phys Rev E 76:041–507. doi:10.1103/PhysRevE.76.041507

Phan VN, Nguyen NT, Yang C, Joseph P, Djeghlaf L, Bourrier D, Gue AM (2010) Capillary filling in closed end nanochannels. Langmuir 26:13–251. doi:10.1021/la1010902

Pipe C, McKinley G (2009) Microfluidic rheometry. Mech Res Commun 36:110–120. doi:10.1016/j.mechrescom.2008.08.009

Radiom M, Chand WK, Yang C (2010) Capillary filling with the effect of pneumatic pressure of trapped air. Microfluid Nanofluid 9:65–75. doi:10.1007/s10404-009-0527-1

Saha AA, Mitra SK (2009) Effect of dynamic contact angle in a volume of fluid (VOF) model for a microfluidic capillary flow. J Colloid Interface Sci 339(2):461–480. doi:10.1016/j.jcis.2009.07.071

Srivastava N, Burns MA (2006) Analysis of non Newtonian liquids using a microfluidic capillary viscometer. Anal Chem 78:1690–1696. doi:10.1021/ac0518046

Srivastava N, Davenport RD, Burns MA (2005) Nanoliter viscometer for measuring blood plasma. Anal Chem 77:383–392. doi:10.1021/ac0494681

Waghmare PR, Mitra SK (2012) A comprehensive theoretical model of capillary transport in rectangular microchannels. Microfluid Nanofluid 12:53–63. doi:10.1007/s10404-011-0848-8

Washburn EW (1921) The dynamics of capillary flow. Phys Rev 17:273–283. doi:10.1103/PhysRev.17.273

White F (1998) Fluid Mechanics. McGraw-Hill, New York